論文 / 著書情報
Article / Book Information

Title	EXPERIMENTAL STUDY OF A BRACE-TYPE VISCOELASTIC DAMPER UNDER LONG-PERIOD AND LONG-DURATION EXCITATIONS
Authors	D. M. Osabel, D. Sato, K. Kasai
Pub. date	2020, 9
Citation	2020 17WCEE Proceedings

17th World Conference on Earthquake Engineering, 17WCEE
Sendai, Japan - September 13th to 18th 2020

EXPERIMENTAL STUDY OF A BRACE-TYPE VISCOELASTIC DAMPER UNDER LONG-PERIOD AND LONG-DURATION EXCITATIONS

D.M. Osabel [(1)], D. Sato [(2)], and K. Kasai [(3)]

[(1)] *Graduate student, Architecture and Building Engineering Dept., Tokyo Institute of Technology, osabel.d.aa@m.titech.ac.jp*
[(2)] *Assoc. Prof., Future Interdisciplinary Research of Science and Technology, Tokyo Institute of Tech., sato.d.aa@m.titech.ac.jp*
[(3)] *Professor, Future Interdisciplinary Research of Science and Technology, Tokyo Institute of Tech., kasai.k.ac@m.titech.ac.jp*

Abstract

As buildings become taller, their natural period becomes longer making them more susceptible to long-period earthquakes and long-duration wind loadings. Properly employing viscoelastic (VE) dampers is one effective way of controlling the structural vibrations induced by the aforementioned loadings. These vibration control devices are found to be frequency and temperature sensitive. Their dynamic properties (i.e., damping and stiffness) appear to be high at low temperature and high frequency, and appear to be low at high temperature and low frequency. Brace-type VE dampers are among the common types of installation, and they work by converting the dissipated kinetic energy into small amount of heat. Depending on the several factors, damper temperature can significantly increase, thereby, lowering the dynamic properties. A handful of experimental studies had been conducted in the past to evaluate the dynamic mechanical properties of VE dampers. However, most of these studies consider only few oscillations (e.g., 6 cycles only) wherein the damper temperature may not have increased significantly, a typical case for short buildings under earthquake excitation. In the 2011 Great Tohoku Earthquake, tall buildings in the Kanto Area of Japan continued to sway even after the shaking of the ground had stopped. For such a case, temperature of VE dampers installed can increase drastically. It is, therefore, the objective of this study to investigate the performance of full-scale brace-type VE dampers under long-period earthquake by conducting experiment. Damper deformations applied in the test are based on random vibration wave and on the equivalent-sinusoidal wave calculated using the technique previously proposed by the co-authors. From these tests, it is found that damper temperature increases significantly causing the damper properties to reduce by more than 40%. Moreover, this study also carries out an experimental investigation of VE damper under long-duration harmonic loading such as strong wind. Despite the drastic decrease of damper properties due to several loading cycles, the damper eventually reached steady-state behavior. This is attributed to the heat generated being transferred to the surrounding air, limiting the rise of damper temperature. With the damper reaching thermal equilibrium, the damper properties become constant. The findings in this paper are essentially important in the design and modeling of VE dampers for tall building installations.

Keywords: viscoelastic damper; long-period earthquake; long-duration loading; damper property degradation

1. Introduction

1.1 High-rise Buildings against Long-Period and Long-Duration Excitations

High-rise buildings are among the defining components in the landscape of big metropolitan cities. With their towering heights and light-weight construction materials, they are more susceptible to wind loadings than medium-rise buildings. In cities frequently struck by typhoon such as Tokyo, Japan, high-rise buildings are designed to withstand strong wind which are long-duration loadings. In addition, these high-rise buildings must be designed to perform well under earthquake.

The recent 2011 Great East Japan Earthquake has brought the attention of many researchers and engineers to investigate the actual responses of high-rise buildings against the long-period ground motion [e.g., 1-3]. The said earthquake was felt as far as Tokyo, Nagoya and Osaka [1] with ground motion records showing short- to long-period components. As reported by Kasai *et. al* [2], high-rise buildings in Tokyo responded mainly due to the predominant long-period component.

1.2 Viscoelastic Dampers

Passive-control devices, such as viscoelastic (VE) dampers, can improve the performance of high-rise buildings by providing supplemental damping [4]. VE dampers are fundamentally made by sandwiching VE material between steel plates as in Fig. 1a. They dissipate the kinetic energy through shear deformation of the VE material, and converts the dissipated energy into small amount of heat. Depending upon several factors (e.g., low thermal conductivity of the VE material, loading duration, and damper configuration), the generated heat can be accumulated within the VE material. For such a case, the damper temperature will increase significantly, softening the VE material and decreasing the dynamic mechanical properties of the damper. These dynamic properties can be determined from the typical elliptical curve of force-deformation shown in Fig. 1b, i.e., storage stiffness $K'_d = F'_d/u_{d0}$ and loss stiffness $K''_d = F''_d/u_{d0}$, where F'_d and F''_d are the forces at the maximum deformation u_{d0} and zero deformation, respectively.

Viscoelastic dampers can be installed in a number of ways. Some of the common installations in Japan are shown in Fig. 2 [5-6]. The frames with brace type (Fig. 2a) and shear link type (Fig. 2b) installations are considered to be a directly connected system where dampers are effective in directly controlling the drifts of the frame. On the other hand, the frame with stud panel type installation (Fig. 2c) is an indirectly connected system where dampers are generally less effective than those previously mentioned system [5].

1.3 Objectives and Scope

Despite the increasing popularity of brace-type viscoelastic damper as a passive-control device for high-rise buildings, there are only a handful of experimental studies on this type of VE damper. Most of these experimental studies were focused on typical earthquake excitation considering only few loading cycles (e.g.,

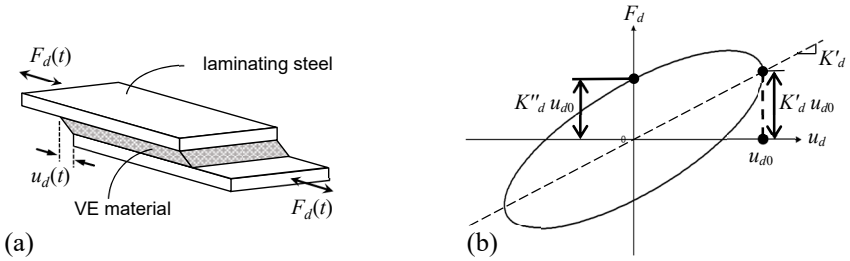

Fig. 1 – (a) Schematic configuration of a viscoelastic damper, and (b) typical force-deformation curve.

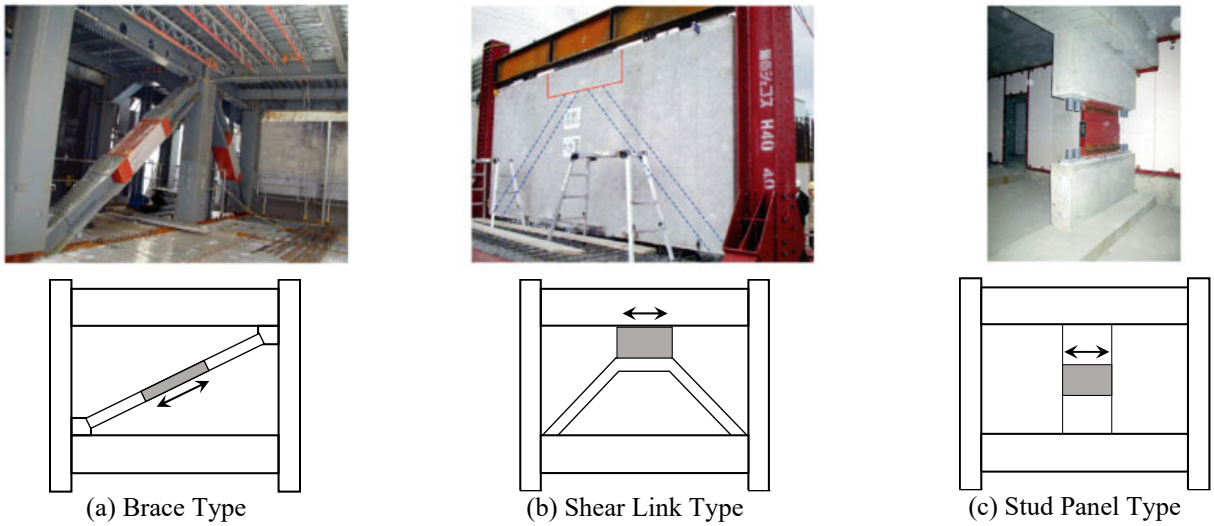

(a) Brace Type (b) Shear Link Type (c) Stud Panel Type

Fig. 2 – Different VE damper installations (Photos are from Ref [6]).

6 cycles). As mentioned above, high-rise buildings are susceptible to both long-period ground motion and long-duration loading such as wind. This motivates the researchers to test a full-scale brace-type VE damper for the aforementioned loadings. In order to properly evaluate the dynamic properties of VE dampers for random loading, the equivalent-sinusoidal wave [7] was adopted. In addition, tests were conducted at different ambient temperatures in order to grasp the effect of initial temperature.

2. Damper Specimen, Test Setup and Loading Conditions

2.1 VE Damper Test Specimen and Test Setup

Two full-scale brace-type VE dampers were used in this study. Table 1 indicates the specifications of the VE dampers used for each test. The dampers were made of 3M-ISD111 type VE material with the material properties: shear modulus $G = 3.92$ N/cm2, fractional derivative order $\alpha = 0.558$, at reference temperature $\theta_{ref} = 20.0°C$, $a_{ref} = 0.0056$ and $b_{ref} = 2.10$, and $p_1 = 14.06$ and $p_2 = 97.32$.

The specimens were tested by applying a displacement-control axial loading along the longitudinal axis (X-axis) as shown in Fig. 3. The deformation of the horizontal slider $u_s(t)$ was desired to be equal to twice that of the dynamic actuator $u_{act}(t)$ by using an amplification mechanism with a factor of 2. The damper deformation $u_d(t)$, which refers to the VE material shear deformation (Fig. 4a), was measured using displacement transducers.

The axial strain of the steel brace was measured using 6 strain gages with locations shown in Fig. 4b. Strain measurement was carried out at 0.01-second interval for Test-01 and at 0.02-second interval for Test-02. The average of the measured strains at any given time instance was calculated and then used to determine the reaction force $F_d(t)$ of the VE damper. Also, temperatures at different locations, on the steel surface and inside the VE material (Fig. 4c), were measured using thermocouples. Temperature measurement was carried out at every 1.0 second for both Test-01 and Test-02.

Table 1 – Full-scale viscoelastic damper specimen specifications

Test	Damper Specimen	Length l (mm)	Total shear area A_s (cm^2)	Thickness of one VE lamination t_{VE} (mm)	Number of laminations
Test-01	VE01	4024.5	9120.0	8	6
Test-02	VE02	4024.5	8544.0	8	6

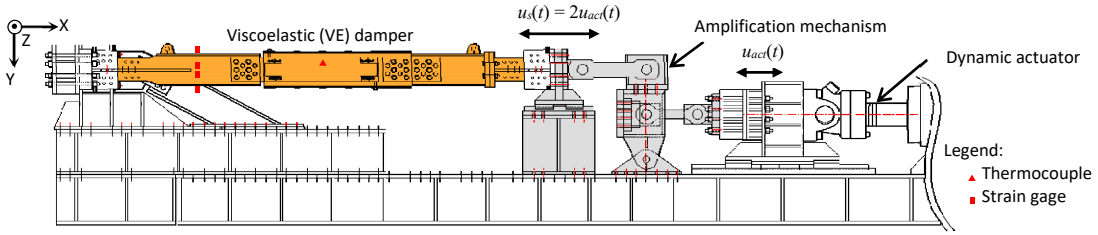

Fig. 3 – Viscoelastic (VE) damper test setup.

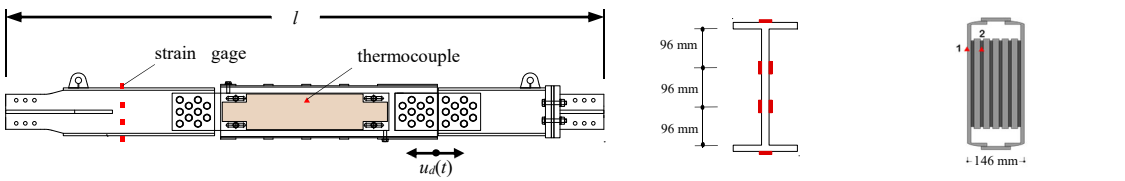

(a) VE damper side view (b) Strain gage positions (c) Thermocouple positions

Fig. 4 – Measurement locations for the test setup.

2.2 Test Conditions and Dynamic Loading

2.2.1 Test-01: Long-Period Excitation (Earthquake)

There were two displacement-control loading protocols used for Test-01, i.e., random and sinusoidal deformations. These were determined as follows: A multi-degree-of-freedom (MDOF) model of a 30-story high-rise building (height = 128 m) with damping ratio of 10% was considered. It was subjected to a long-period ground motion and response history analysis was performed. The inter-story drift δ history of each layer was determined, and the response of the layer with the largest maximum value of δ and with the largest standard deviation of δ was considered to determine the displacement-control loading protocol.

Considering brace-type installation of VE dampers, random damper deformation $u_d = \delta \cdot cos\beta$, where β is the mounting angle of the VE damper. Assuming that $\beta = 30° \sim 45°$, it was estimated that $u_d = 0.80\delta$. Applying this relationship to the above mentioned layer response considered to determine the random loading protocol, the time-history of u_d for random deformation was determined and is shown in Fig. 5a.

As for the harmonic loading protocol, it is determined by getting the equivalent sinusoidal-wave of the random damper deformation (Fig. 5a). According to Sato *et al.* [7], the frequency f_r and the amplitude u_d of the equivalent-sinusoidal damper deformation are

$$f_r = N_0^+ / t_a \text{ , and } u_d = \sigma_u \sqrt{2} \text{ .} \qquad \text{(1a, b)}$$

Here, N_0^+ = number of positively-sloped x-intercepts, t_a = loading duration, and σ_u = standard deviation of u.

As seen in Fig. 5a, the magnitude of random damper deformation is not significantly large for the entire duration. Therefore, t_a considered herein is only 65.8 seconds, and accordingly, $N_0^+ = 23$ and $\sigma_u = 17.65$ mm. By Equations 1a and 1b, the harmonic loading protocol for Test-01 (Table 1 and Fig. 5b) has $f_r = 0.35$ Hz (period $T = 2.86$ s) and $u_d = 24.96$ mm (VE material shear strain $\gamma_d = 312\%$).

Ambient temperatures θ_0 for the random and equivalent-sinusoidal loading cases of Test-01 were 22°C.

2.2.2 Test-02: Long-Duration Excitation (Wind)

For Test-02, only harmonic loading protocol was used to excite specimen VE02 (Table 2). It was decided that $T = 4.00$ s and $u_d = 20.00$ mm ($\gamma_d = 250\%$). Loading duration was 21,600 seconds (or 6 hours) which translates to a total of 5400 loading cycles. The ambient temperature θ_0 was 6°C.

Table 2 –Test Conditions and Harmonic Loading (Equivalent Sinusoidal Wave)

Test	Ambient Temp. θ_0 (°C)	Period T (s)	Amplitude u_d (mm)	Duration t_0 (s)	Number of cycles
Test-01	22	2.86	24.96	65.8	23
Test-02	6	4.00	20.00	21600.0	5400

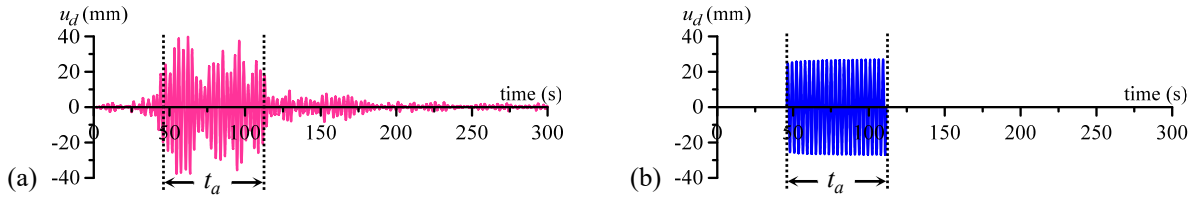

Fig. 5 – Dynamic loading protocols for Test-01: (a) Random damper deformation from the time-history analysis of MDOF subjected to long-period earthquake, and (b) the calculated equivalent sinusoidal-wave.

3. Experimental Results

3.1 Test-01 Results

Fig. 6 shows the results for Test-01 under long-period excitations (random and equivalent-sinusoidal waves). From the time-history plots in Fig. 6a of the temperature θ measured at the surface of steel and inside one of the VE laminations (points 1 and 2, respectively, from Fig. 4c), it is seen that the temperature-rise from the equivalent-sinusoidal wave test has good correlation to that of the original random loading. From the initial temperature of about 22°C, the temperature at the VE lamination (point 2) reached a maximum of 34.80°C for the random loading and 36.10°C for the equivalent sinusoidal wave.

As shown in Fig. 6b, it is unclear to see any correlation in the damper forces F_d of random and sinusoidal loading cases. Instead, the wave pattern of the F_d time-history has strong correlation with the deformation u_d (Fig. 5). By looking at the F_d result of the random loading case, it is uncertain to grasp any decrement of VE damper capacity due to the increase of temperature (Fig. 6a). In contrast, the decrement of the VE damper capacity is clearly noticed in the F_d time-history of the sinusoidal loading case, i.e., from peak value of F_d = 394.05 kN in the first, decreasing gradually to F_d = 172.58 kN in the last cycle.

In addition to the similarity of temperature-rise (Fig. 6a), it is necessary to verify the equivalence of the random and sinusoidal loading cases by directly inspecting the VE damper performance using the cumulative dissipated energy W_d. Accordingly, the dissipated energy $W_d^{(i)}$ at every time-step i is

$$W_d^{(i)} = \left(F_d^{(i+1)} + F_d^{(i)}\right)\left(u_d^{(i+1)} - u_d^{(i)}\right)/2 \tag{2}$$

where $F_d^{(i)}$ and $u_d^{(i)}$ are the damper force and deformation at time-step i, respectively.

From the cumulative dissipated energy shown in Fig. 7, it is verified that the VE damper performs similarly when under random loading and equivalent-sinusoidal loading (calculated using Equation 1 [7]).

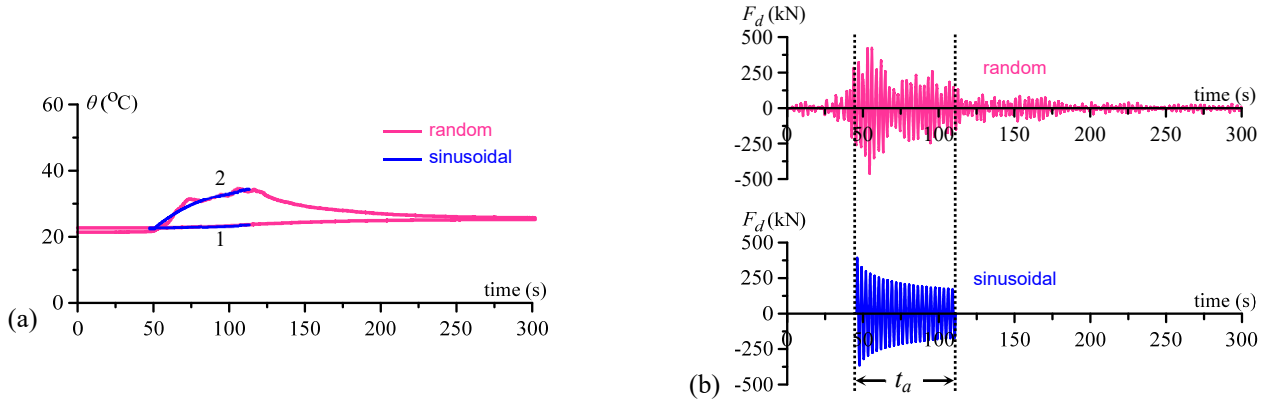

Fig. 6 –Time-history results of Test-01: (a) temperature θ, and (b) damper force F_d.

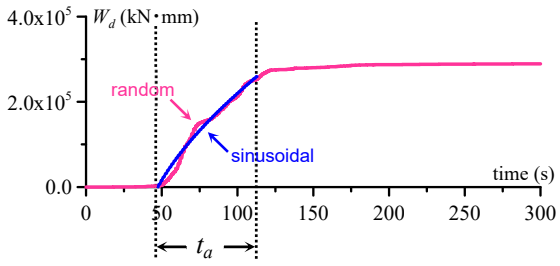

Fig. 7 – Cumulative dissipated energy W_d for Test-01: random wave vs. equivalent sinusoidal-wave.

Under random loading, significant amount of energy is dissipated during the duration t_a. Outside this time-range, W_d plot is almost horizontal. With this verification, the results of Test-01 under sinusoidal loading will be utilized later in Chapter 4 when comparing with Test-02 results.

3.2 Test-02 Results

Fig. 8a shows the time-history of the temperatures θ on the surface of steel and inside VE material for Test-02. Temperatures were recorded during the application of the harmonic loading (i.e., for 21,600 seconds or 6 hours), and continued even after the loading. During the application of loading, heat was continuously generated for 5400 cycles, thus, significantly increasing the damper temperature. Most of the heat is accumulated in the laminated VE materials because of its low thermal conductivity. From initial temperature of 6°C, the maximum recorded temperature inside the VE lamination (point 2) is 59.63°C and on the steel part (point 1) is 34.46°C after the 6 hours. Upon the termination of the harmonic loading, heat generation immediately stopped. Thereafter, the damper temperature decreases as the heat retained inside the damper is transferred to the surrounding air. However, it takes a long time for the bring down the damper temperature to its initial condition.

Moreover, the heat transfer aspect particularly in the first few loading cycles is investigated. Fig. 8b shows a closer look into the temperature of Test-02 for t = 0 to 300 seconds, and Fig. 8c shows the slope of the temperature-rise. Immediately after the initiation of loading, the temperature inside the VE lamination (point 2) increases abruptly – manifested by a relatively steep slope. As the loading progressed, the heat generated within the VE material is transferred to other parts (e.g., steel plates), thus, the rate of temperature-rise gradually decreases while the temperature of steel (point 1) gradually increases. Eventually at about t = 75 seconds, the rates of temperature-rise on the steel plate (point 1) and inside the VE material (point 2) are almost the same. This slow rate of increase of temperature-rise in the steel is due to the low thermal conductivity of VE material. The heat generated within the VE material takes a significant amount of time to travel to the steel plate. With heat continuously generated, heat accumulates inside the VE material.

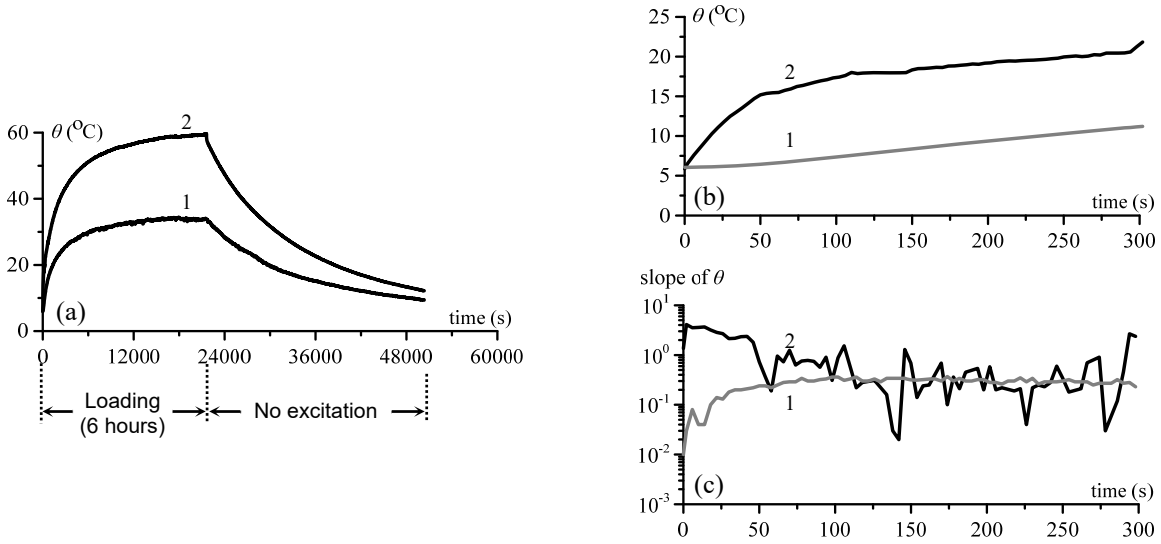

Fig. 8 – Test-02 Temperature results: (a) time-history for the entire duration of measurement, (b) history from time t = 0 s to 300 s, and (c) rate of temperature-rise.

4. VE Damper Performance

This chapter evaluates the performance of the VE dampers under long-period and long-duration excitations based on the harmonic loading tests. As discussed in the Section 3.1, the sinusoidal loading case of Test-01 is verified to be equivalent to that of random loading case.

4.1 Hysteresis loop

As mentioned in Section 1.2, the dynamic properties of VE damper can be estimated from the force-deformation hysteresis loop (Fig. 1b). The fatness and slope of the hysteresis loop describe the damping and stiffness of the VE damper, respectively. However, since a VE damper has relatively high initial stiffness and there is possible machine-caused-error at the initiation of the dynamic actuator, a number of test data at the start has to be ignored. Therefore, a cycle of the hysteresis loop must be defined explicitly.

Fig. 9a shows half waves 1 to 3. Half wave 1 is from point *o* to point *p*, half wave 2 is from point *p* to point *q*, and half wave 3 is from point *q* to point *r*. This paper defines cycle 1 by neglecting half-wave 1 and considers the combinations of half wave 2 and half wave 3 only. Not shown here, but it follows that cycle 2 is composed of half wave 4 and half wave 5. At the end of loading duration, test data is checked to verify the that the final cycle is complete and free from error.

With the above definition, the $F_d - u_d$ curves for Test-01 and Test-02 are obtained. Fig. 9b shows all the 21 cycles of Test-01 while Fig. 9c shows cycles 1~21 and 5388~5398 of Test-02. Comparing cycles 1~21 of from these figures, the hysteresis loops of Test-02 are generally fatter and steeper than those corresponding loops of Test-01. This signifies the temperature sensitiveness of VE material. Since specimen VE02 of Test-02 was tested at low ambient temperature of 6°C, its VE material was initially stiffer than the VE01 tested at 22°C ambient temperature.

As the loading continues, the hysteresis loops for both tests (Figs. 9b and 9c) become slimmer with declining slope due to the increase of damper temperature (Chapter 3). However, VE02 of Test-02 was continually subjected to more loading cycles (long-duration excitation) causing its hysteresis loops to decline furthermore. For cycles 5388~5398, its hysteresis loops are relatively very small compared to cycle 1 due to large increase of damper temperature (Fig. 8a).

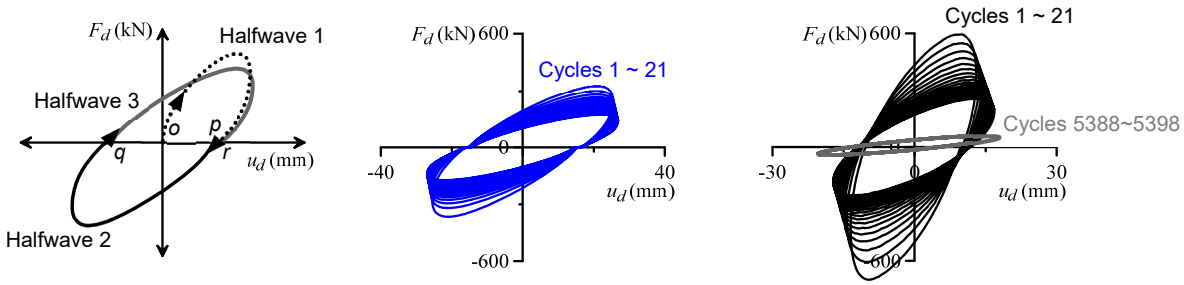

(a) Definition of Cycle 1 (b) Test-01 (c) Test-02

Fig. 9 – Hysteresis loops.

4.2 Dissipated Energy of VE Damper

The dissipated energy per cycle $W_d^{[n]}$ can be calculated from the area of hysteresis loop (Fig. 9) for each cycle. Accordingly,

$$W_d^{[n]} = \sum_{j=1}^{N_D} \frac{\left(F_d^{(j+1)} + F_d^{(j)}\right)\left(u_d^{(j+1)} - u_d^{(j)}\right)}{2} \tag{3}$$

where N_D refers to the number of data in cycle n, and j refers to the time-step in the cycle considered.

Fig. 10a shows the values of $W_d^{[n]}$ for Test-01 and Test-02 (first 25 cycles). Overall, Test-02 with low ambient temperature has higher amount of dissipated energy per cycle. This is because the enclosed area per

cycle in the hysteresis loop of Test-02 (Fig. 9c) is bigger than those of Test-01 (Fig. 9b). The two tests have almost the same peak deformations per cycle but Test-02 has fatter loop since it was tested at low ambient temperature.

Due to the heat generated from dissipating kinetic energy, the performance of VE dampers decreased immediately after one cycle. Fig. 10b shows that the rates at which the amount of dissipated energy per cycle decrease for both tests are almost the same for the first 7 cycles. Thereafter, Test-01 decreases at a slower rate than Test-02, and ended with $W_d^{[21]}$ which is 0.60 times $W_d^{[1]}$.

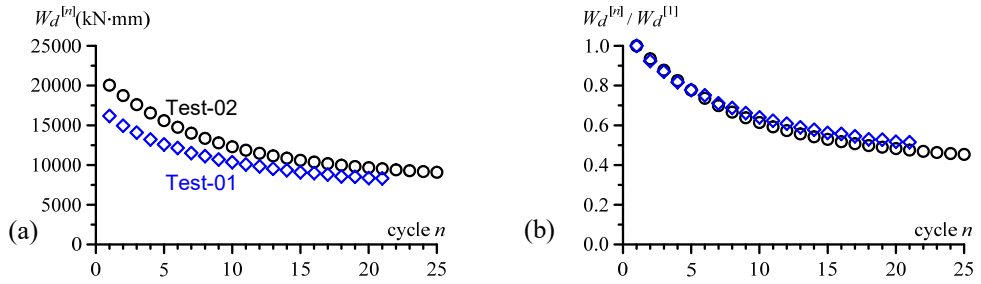

Fig. 10 – (a) Dissipated energy W_d and (b) normalized value per cycle.

4.3 Peak Damper Force

The peak damper force $F_d^{[n]}$ for each cycle is calculated as the average of the positive and negative peak damper forces in one cycle. As seen in Fig. 11a, $F_d^{[1]}$ of Test-01 is only about 0.50 times that of Test-02. However, at cycle 21, its peak damper force is about 0.75 times that of Test-02. Its $F_d^{[n]}$ values decrease at a lower rate than that of Test-02. As seen in the normalized value per cycle (Fig. 11b), peak damper force of Test-01 at cycle 21 (end of loading) is about 0.50 times its initial value, whereas peak damper force of Test-02 at cycle 21 is about 0.40 times its initial value.

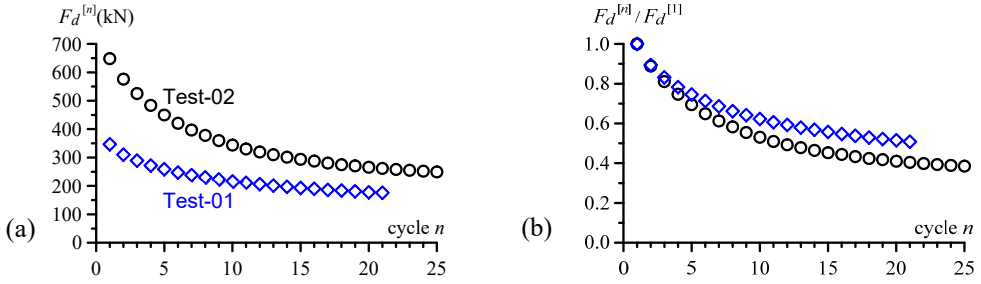

Fig. 11 – (a) Peak damping force F_d and (b) normalized value per cycle.

4.4 Storage Stiffness and Damping Coefficient

The storage stiffness K'_d and damping coefficient C_d per cycle are calculated as follows:

$$K'_d = \frac{N_D \Sigma \left(u_d^{(j)} \cdot F_d^{(j)}\right) - \Sigma u_d^{(j)} \Sigma F_d^{(j)}}{N_D \Sigma \left(u_d^{(j)}\right)^2 - \left(\Sigma u_d^{(j)}\right)^2} \quad \text{, and} \quad C_d = \frac{\eta_d K'_d}{(2\pi f)} \tag{4a, b}$$

where loss factor η_d is calculated as

$$\eta_d = \frac{W_d}{\pi K'_d (u_{d0})^2} \quad . \tag{5}$$

Figs. 12a and 13a show the storage stiffness K'_d and damping coefficient C_d of the tests, respectively. From these figures, the cycle 1 values of K'_d and C_d for Test-01 are 0.33 and 0.20 times the corresponding cycle 1 values that of Test-02. Unlike in Sections 4.2 and 4.3 where the normalized values $W_d^{[n]}$ and $F_d^{[n]}$, respectively, for both tests are almost the same, the pattern for the normalized values of K'_d and C_d is different from above. As in Figs. 12b and 13b, the normalized values of K'_d and C_d for Test-02 are lower than those for Test-01.

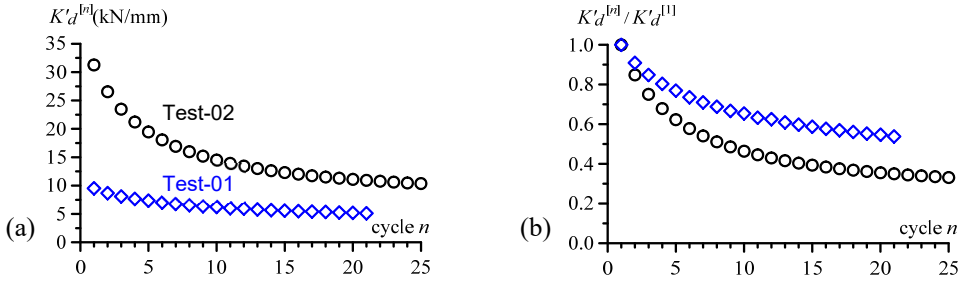

Fig. 12 – (a) Storage stiffness K'_d and (b) normalized value per cycle.

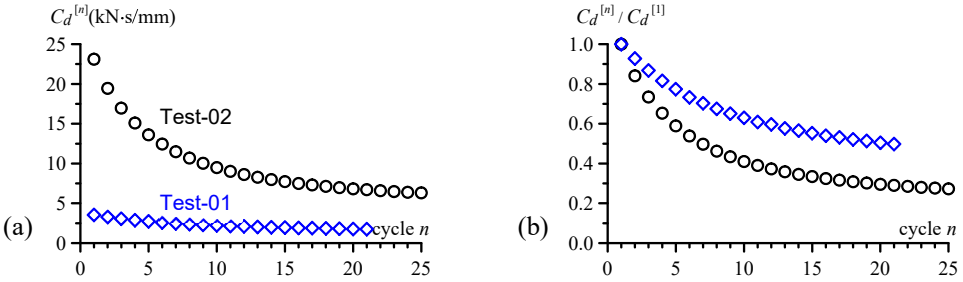

Fig. 13 – (a) Damping coefficient C_d and (b) normalized value per cycle.

From these results, VE dampers in a low ambient temperature tend to have a larger property decrement than those in a warm ambient temperature. Since VE material the initial properties of VE damper at low ambient temperature are relatively high, it dissipates a large amount of energy and the amount of heat generated is also high. This in turn will result to a 70% reduction of dynamic properties after 20~25 loading cycles only.

4.5 Behavior under Long-Duration Excitation

Fig. 14 shows the relationship between the increase of VE damper temperature and the decrease of the storage stiffness for Test-02. A large amount of heat is accumulated inside the VE damper causing the VE material to soften, thus, the dynamic property (e.g., K'_d) decrease by 93%. However, as seen in the figure below, values of K'_d and θ at point 2 become almost constant despite being subjected to long-duration loading. This is because as the VE material softens, the amounts of dissipated energy and heat generated are becoming small. Since heat is continuously dispersed to the surrounding air, the amount of heat generated becomes almost be the same as the heat transferred to the air. As such, the VE damper responded in a steady-state behavior.

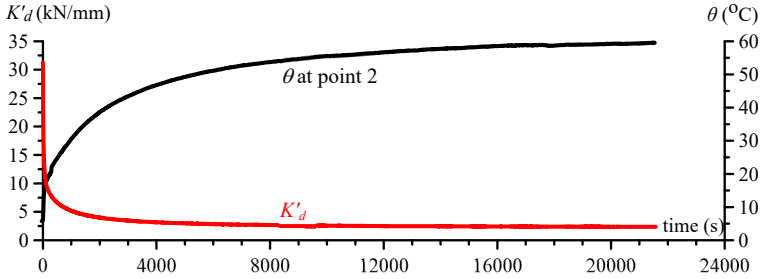

Fig. 14 – Test-02: Storage stiffness K'_d and temperature inside VE material for the entire loading duration.

5. Conclusions

From this study, the following findings are drawn:

1. Naturally, structural vibrations induced by ground motion and wind are random but the decrement of damper properties can be fully grasped if loadings are sinusoidal waves. Thus, a method of getting an equivalent sinusoidal-wave proposed by the co-authors was adopted. The dissipated energy of the VE damper under the random and the equivalent-sinusoidal were identical, verifying the use of sinusoidal loading for the investigation of VE damper behavior.
2. Immediately upon loading, the temperature inside the VE material increases. However, due to the low thermal conductivity of the VE material, it will take a number of loading cycles before the heat is transferred to the laminating steel plates. This leads to heat accumulating within the VE material.
3. VE dampers installed on high-rise buildings subjected to long-period ground motion will tend to oscillate 20~23 cycles. This will cause the damper temperature to have significant increase, thus, significant reduction of dynamic properties is inevitable.
4. The ambient temperature (vis-à-vis initial temperature of the VE damper) greatly affects how the VE damper behaves. At low ambient temperature, dynamic properties tend to reduce more than at high ambient temperature.
5. Due to continuous heat transfer to the surrounding air and due to the decrease of the dissipated energy as the VE material becomes warm, the VE damper will eventually behave in a steady-state manner despite being subjected to the long-duration loading.

Acknowledgements

This work was supported by the JST Program on Open Innovation Platform with Enterprises, Research Institute and Academia. We are also grateful to Assoc. Prof. Kazuhiro Matsuda (Meijo University, Japan), and to Mr. Sho Nagayama and Mr. Nobumasa Sugiyama (former graduate students of Tokyo Institute of Technology) for providing invaluable information vital for this paper. We also acknowledge the help of Mr. Hitoshi Takimoto and Mr. Fumiya Ueno (graduate students of Tokyo Institute of Technology, Japan) in the preparation and conduct of the experiment.

References

[1] Takewaki I, Murakami S, Fujita K, Yoshitomo S, and Tsuji M (2011): The 2011 of the Pacific Coast of Tohoku Earthquake and Response of High-Rise Buildings under Long-Period Ground Motions. *Soil Dynamics and Earthquake Engineering*, 31, 1511-1528

[2] Kasai K, Pu W, and Wada A (2012): Responses of Controlled Tall Buildings in Tokyo subjected to the Great East Japan Earthquake. In: *Proceedings of the International Symposium on Engineering Lessons Learned from the 2011 Great East Japan Earthquake*, March 1-4, 2012, Tokyo, Japan, p. 1099-1109.

[3] Takewaki I, Fujita K, and Yoshitomo S (2013): Uncertainties in Long-Period Ground Motion and Its Impact on Building Structural Design: Case study of the 2011 Tohoku (Japan) Earthquake. *Engineering Structures*, 49, 119-134.

[4] Chopra AK (2012): *Dynamics of Structure: Theory and Applications to Earthquake Engineering* (4th ed.). Prentice Hall.

[5] Kasai K, and Kibayashi M (2004): JSSI Manual for Building Passive Control Technology Part 1: Manual Contents and Design/Analysis Methods. Proceedings: *13th World Conference on Earthquake Engineering*, Paper No. 2989, August 1-6, 2004, Vancouver, Canada.

[6] Kibayashi M, Kasai K, Tsuji Y, Kikuchi M, Kimura Y, Kobayashi T, Nakamura H, and Matsuba Y (2004): JSSI Manual for Building Passive Control Technology Part 2: Criteria for Implementation of Energy Dissipation Devices. Proceedings: *13th World Conference on Earthquake Engineering*, Paper No. 2990, August 1-6, 2004, Vancouver, Canada.

[7] Sato D, Tokoro K, Kasai K, Kitamura H (2015): Properties of Viscoelastic Damper under Wind-Induced Excitation and Simplified Evaluation Method using Sinusoidal-Wave. *J. Struct. Constr. Eng.* AIJ, 80(710), 571-581 (In Japanese).

